

Microarray data reveal potential genes that regulate triple-negative breast cancer

Journal of International Medical Research
2022, Vol. 50(10) 1–15
© The Author(s) 2022
Article reuse guidelines:
sagepub.com/journals-permissions
DOI: 10.1177/03000605221130188
journals.sagepub.com/home/imr



Chi Pan^{1,*}, Aihua Cong^{2,*} and Qingtao Ni² 

Abstract

Objective: Triple-negative breast cancer (TNBC) is characterized by a lack of targeted therapies and poor patient prognosis, and its underlying pathological mechanisms remain unclear. This study aimed to identify potential key genes and related pathways that are required for TNBC development.

Methods: We screened the Gene Expression Omnibus database for transcriptome data and identified differently expressed genes in TNBC. Then, we performed Gene Ontology analysis to determine the genes and pathways involved in TNBC development. We correlated significantly expressed genes and miRNAs using miRDB, TargetScan, miRWalk, and DIANA, and then validated the expression of CDK1 and miR-143-3p in TNBC patients.

Results: Eighteen genes were significantly upregulated in TNBC patients, and these were found to be enriched in cell metabolic process, cell division, mitochondrion, and respiratory chain. MiR-143-3p was found to be an upstream regulator of CDK1. Validation experiments revealed that CDK1 was upregulated while miR-143-3p was downregulated in clinical TNBC specimens.

Conclusions: Collectively, our results revealed 18 upregulated genes in TNBC. Notably, CDK1 and its related microRNA miR-143-3p could be potential therapeutic targets for TNBC.

Keywords

Bioinformatics, CDK1, key genes, miR-143-3p, triple-negative breast cancer, cell cycle

Date received: 5 April 2022; accepted: 15 September 2022

*These authors contributed equally to this work.

Corresponding author:

Qingtao Ni, Department of Oncology, Jiangsu Taizhou People's Hospital, Hailing South Road 399, Taizhou 225300, China.
Email: nqt1990@126.com

¹Department of General Surgery, Jiangsu Taizhou People's Hospital, Taizhou, China

²Department of Oncology, Jiangsu Taizhou People's Hospital, Taizhou, China



Introduction

Breast cancer (BC) has high incidence and mortality rates in women. Estimates from the United States indicate that approximately 284,200 new BC cases are expected in women annually, of which 44,130 patients are likely to die.¹ The prognosis of BC patients has markedly improved, owing to improved approaches for early diagnosis, surgery, neoadjuvant chemotherapy, and molecular targeted gene therapy. Studies have shown that up to 10% of BC cases originate from genetic mutations.² In addition to BRCA1/2, the expression of protein kinase R (PKR) and phosphatidylinositol 4-kinase 2-alpha (PI4K2A) have been shown to play important roles in the prognosis of BC patients.³ Studies have also shown that inhibiting the activity of fatty acid transport protein 1 (FATP1) can inhibit the ability of BC cells to obtain fatty acids, thereby suppressing cell viability.⁴ Results from *in vitro* experiments have revealed that combining a highly specific anti-human epidermal growth factor receptor 3 (HER3) antibody with siRNAs can effectively inhibit the proliferation of HER3-positive BC cells.⁵ Triple-negative breast cancer (TNBC) is a subtype of BC that accounts for between 10% and 15% of all cases. To date, no effective targeted therapy has been developed for TNBC.⁶ Therefore, searching for potential

molecular targets is crucial to providing a theoretical basis that will guide the development of effective molecular targeted therapies for TNBC.

Bioinformatics analyses have been widely used to identify differentially expressed genes (DEGs) and related signaling pathways with the aim of improving disease diagnosis and drug discovery. In this study, we aimed to identify DEGs in TNBC on the basis of three microarray datasets from the Gene Expression Omnibus (GEO) database. Subsequently, we performed Gene Ontology (GO) pathway enrichment and functional analyses to reveal the molecular mechanisms underlying TNBC development and identify therapeutic targets. The workflow of this study is summarized in Figure 1.

Methods

Analysis of gene microarray data

To identify important genes involved in TNBC, we selected and downloaded three gene expression datasets for BC, namely GSE57297, GSE65212, and GSE38959 from the GEO database (<http://www.ncbi.nlm.nih.gov/geo>). The GSE57297 dataset comprises three TNBC samples alongside seven healthy controls, GSE65212 comprises 55 and 11 TNBC and healthy samples,

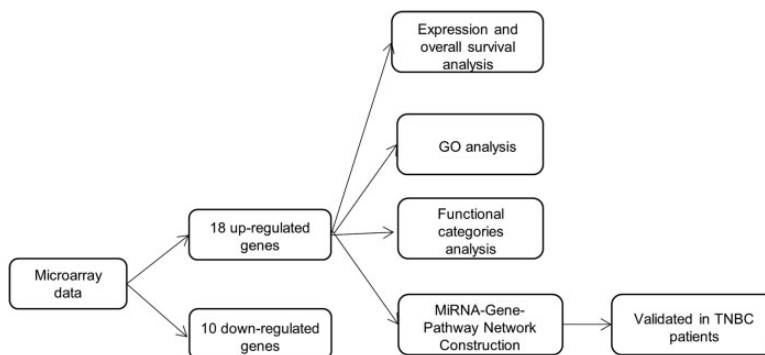


Figure 1. Workflow of the analysis performed in this study.

respectively, and GSE38959 has 30 TNBC samples alongside three healthy controls. We employed GEO2R (<http://www.ncbi.nlm.nih.gov/geo/geo2r>) to identify DEGs in BC samples relative to controls using the thresholds p -adjusted value <0.05 and $\log_{2}FC$ (fold change) >1 . Next, we queried the gene expression profiling interactive analysis (GEPIA2) database (<http://gepia.cancer-pku.cn/>) for full names of the genes and their expression profiles in BC.

GO pathway analysis of the identified DEGs

Functional annotation of identified genes was performed using the DAVID database (<http://david.ncifcrf.gov/>) at a statistical significance of $P < 0.05$.

Differential gene expression and survival analyses

Analyses of differential gene expression and survival analyses according to gene expression were conducted using the starBase online platform (ENCORI Pan-Cancer Analysis Platform, <https://starbase.sysu.edu.cn/panCancer.php>).

MicroRNA identification and network construction

We predicted potential targets of microRNAs using the online prediction tools miRDB (<http://mirdb.org/>), TargetScan (<http://genes.mit.edu/targetscan/>), miRWalk (<http://www.umm.uniheidelberg.de/apps/zmf/mirwalk/>), and DIANA (<http://diana.imis.athena-innovation.gr/DianaTools/>). Subsequently, miRNA–gene–pathway networks were constructed and presented as Venn diagrams (<http://bioinformatics.psb.ugent.be/webtools/Venn/>).

Patients and clinicopathological features

Formalin-fixed and paraffin-embedded (FFPE) samples alongside normal tissues

were obtained from the primary tumors of TNBC patients who were recruited at Jiangsu Taizhou People's Hospital between January 2018 and March 2021. Patients were included in the study if they met the following criteria: (1) underwent surgery for the first time; (2) had not received either chemotherapy or radiotherapy; and (3) voluntarily provided verbal informed consent for use of their FFPE samples. Conversely, patients with any serious medical conditions were excluded from the study. The patients' ages ranged from 28- to 70-years-old (mean: 52.0 years), and disease grades were categorized according to the American Joint Committee on Cancer (AJCC) 8th TNM classification. The study was approved by the Human Ethics Review Committee of Jiangsu Taizhou People's Hospital (KY2021-043-01; 2021-04-16). Because all FFPE samples were from patients treated at Jiangsu Taizhou People's Hospital and remained at the institution, written informed consent was exempted by the Ethics Committee.

RNA extraction and gene expression analysis

FFPE TNBC specimens were sectioned at 10- μ m thickness. RNA was extracted using the miRNAprep Pure FFPE Kit (cat. No. DP502; TianGen Biotech, Beijing, China) in accordance with the manufacturer's instructions, and then reverse transcribed to complementary DNA (cDNA) using the miRcute Plus miRNA First-Strand cDNA Synthesis Kit (TianGen Biotech). The cDNA was subjected to quantitative real-time PCR (qPCR) targeting miR-143-3p using the miRcute Plus miRNA qPCR Detection Kit (TianGen Biotech) on an ABI 7500 system (Thermo Fisher Scientific, Waltham, MA, USA). U6 was used as an internal reference. The real-time reaction for CDK1 was performed using FastKing gDNA Dispelling RT SuperMix (TianGen Biotech). A standard SYBR Green PCR

Kit (Lifeint, Beijing, China) was used to examine mRNA expression in accordance with the manufacturer's protocol. Relative expression was calculated using the $2^{-\Delta Cq}$ method, where $\Delta Cq = Cq(\text{target}) - Cq(\text{reference})$. The primers used were as follows: miR-143-3p forward: 5'-GCGCGTGAGATGAAGCACTGTAGCTC-3'; The reverse primer was the universal primer in the kit; CDK1 forward: 5'-GGTTCCTAGTACTGCAATTTCG-3' and CDK1 reverse: 5'-TTTGCCAGAAATTCGTTTGG-3'; GAPDH forward: 5'-GGAGCGAGATCCCTCCAAAT-3' and GAPDH reverse: 5'-GGCTGTTGTCATACTTCTCATGG-3'. All miRNA primers were obtained from TianGen Biotech. GAPDH was included as an internal reamplification control. The primers were synthesized by Sheng Gong Inc. (Shanghai, China). All experiments were performed in triplicate.

HEK293T cell culture and co-transfection

HEK293T cells were first inoculated in Dulbecco's modified Eagle's medium (DMEM) supplemented with 10% fetal bovine serum (FBS) and 100 U/mL penicillin/streptomycin, and then seeded into six-well plates. A miR-143-3p mimic or miR-negative control was co-transfected into HEK293T cells with CDK1 wild-type or mutant plasmids, respectively, using Lipofectamine 2000 (Thermo Fisher Scientific) in accordance with the manufacturer's instructions. Cells were harvested 48 hours after transfection and subjected to dual-luciferase reporter assays.

Dual-luciferase assay

Dual-luciferase assays were performed using the Beyotime kit (RG027; Shanghai, China) in accordance with the manufacturer's instructions. Briefly, transfected cells were thoroughly lysed for 20 minutes using an oscillator before detection. Next, 100 μL of

firefly luciferase reagents and 20 μL of samples were added to each well, followed by 100 μL of Renilla luciferase reagents with stirring. Finally, the relative light units were measured.

Statistical analysis

Statistical analyses were performed using PASW Statistics for Windows version 18.0 (SPSS Inc., Chicago, IL, USA) and data are presented as mean \pm standard deviation (SD). Differences in clinical parameters between groups were analyzed using Student's unpaired *t*-tests, whereas expression levels of miR-143-3p and CDK1 were compared between TNBC and adjacent non-tumor tissues using paired *t*-tests. Correlations between miR-143-3p and Ki67 were performed using the Spearman correlation test. Differences of $P \leq 0.05$ were considered statistically significant.

Results

Identification of DEGs in TNBC

Differential expression analysis revealed that 3244, 3870, and 6684 genes were upregulated in the GSE57297, GSE65212, and GSE38959 datasets, respectively. A Venn diagram of these genes showed that 18 upregulated genes were shared among the three datasets (Figure 2a). Summaries of the symbols, full names, and expression profiles in GEPIA2 for the 18 upregulated genes are outlined in Table 1. In total, 3172, 7455, and 3827 downregulated genes were identified in GSE57297, GSE65212, and GSE38959, respectively, of which 10 were shared among the three datasets (Figure 2b).

Functional annotation of the 18 upregulated genes

GO terms showed that the upregulated DEGs were significantly enriched in cell

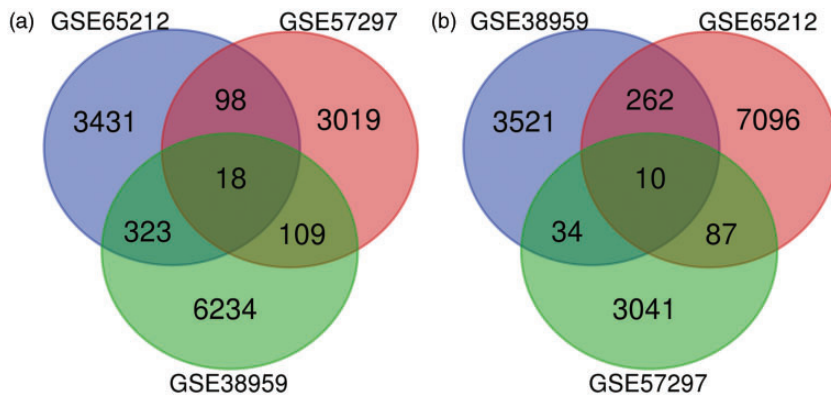


Figure 2. Venn diagram showing DEGs across the three datasets, with an overlap of 18 upregulated genes (a) and 10 downregulated genes (b). DEGs, differentially expressed genes.

Table 1. Summary of the functions of the key upregulated genes in triple-negative breast cancer.

Gene symbol	Full name	Tumor/Normal
OSR2	odd-skipped related transcription factor 2	6.56/18.3
PELO	pelota homolog (Drosophila)	9.67/11.25
NDUFV2	NADH: ubiquinone oxidoreductase core subunit V2	166.81/106.75
TNFSF13B	TNF superfamily member 13b	5.92/2.39
IFI27	interferon alpha inducible protein 27	343.84/268.88
CDK1	cyclin dependent kinase 1	27.89/3.03
WDR83	WD repeat domain 83	10.79/9.89
NDUFS8	NADH: ubiquinone oxidoreductase core subunit S8	125.55/81.49
GNG5	G protein subunit gamma 5	163.83/107.21
GATAD2A	GATA zinc finger domain containing 2A	30.17/23.03
RDH10	retinol dehydrogenase 10 (all-trans)	9.3/12.39
UQCRI0	ubiquinol-cytochrome c reductase, complex III subunit X	128.07/70.98
PSRC1	proline and serine rich coiled-coil 1	7.62/2.68
JMJD4	jumonji domain containing 4	21.12/10.91
PDIA5	protein disulfide isomerase family A member 5	21.47/17.06
PSMD8	proteasome 26S subunit, non-ATPase 8	181.37/135.97
SMARCA4	SWI/SNF related, matrix associated, actin dependent regulator of chromatin, subfamily a, member 4	79.27/43.66
RAB11A	Ras-related protein Rab-11A	225.96/127.22

metabolic process and gene expression (Table 2). Functional GO functional analysis revealed that the DEGs were mainly involved in cell division, mitochondrion, and respiratory chain (Table 3).

Clinical significance of the 18 upregulated genes

Analyses of differential expression and survival data with regards to these genes were

Table 2. GO pathway enrichment analysis of the differentially expressed genes.

Pathway ID	Pathway description	Count in gene set	P-Value
GO:0008152	metabolic process	13	0.034403181
GO:0034641	cellular nitrogen compound metabolic process	11	0.005946409
GO:0006807	nitrogen compound metabolic process	11	0.010284298
GO:0006139	nucleobase-containing compound metabolic process	10	0.011316948
GO:0046483	heterocycle metabolic process	10	0.01320112
GO:0006725	cellular aromatic compound metabolic process	10	0.013955412
GO:1901360	organic cyclic compound metabolic process	10	0.017329052
GO:0010467	gene expression	9	0.025053516
GO:0016070	RNA metabolic process	8	0.041459697
GO:0043933	macromolecular complex subunit organization	7	0.006685346
GO:0048513	animal organ development	7	0.021560177
GO:0006996	organelle organization	7	0.049485402
GO:0006461	protein complex assembly	6	0.003350014
GO:0070271	protein complex biogenesis	6	0.003360225
GO:0071822	protein complex subunit organization	6	0.006351896
GO:0065003	macromolecular complex assembly	6	0.006958666
GO:0016310	phosphorylation	6	0.020989746
GO:0010605	negative regulation of macromolecule metabolic process	6	0.024906105
GO:0031324	negative regulation of cellular metabolic process	6	0.025727529
GO:0009892	negative regulation of metabolic process	6	0.034275727
GO:0022607	cellular component assembly	6	0.03961708
GO:0070887	cellular response to chemical stimulus	6	0.041391773
GO:0007049	cell cycle	5	0.033628604
GO:0009888	tissue development	5	0.039398722
GO:0044093	positive regulation of molecular function	5	0.045733328

Table 3. Functional analysis of the differentially expressed genes.

Pathway description	Count in gene set	%	P-value
Cell division	3	20	0.027775335
Mitochondrion	4	26.67	0.037206541
Respiratory chain	2	13.33	0.042025738

conducted using the starBase online platform. Except for PELO and RDH10, the other 16 genes were upregulated in most BCs (Figure 3a). Kaplan–Meier survival curve analysis demonstrated that there was a significant difference in survival according to the expression of some of the identified genes in BC tissues, including PELO (Figure 3b).

Identification of novel miRNAs

We used miRDB, TargetScan, miRWalk, and DIANA to screen for common targets on the basis of the intersection of elements and visualized the results using a Venn diagram (Figure 4). All four databases contain computationally predicted miRNA–target interactions. Interestingly, only one miRNA (miR-143-3p) was predicted to be an upstream regulator of CDK1 (Figure 4a). Conversely, four miRNAs (miR-5002-5p, miR-6513-5p, miR-942-5p, and miR-6780a-3p) were identified for IFI27 (Figure 4b). Moreover, two miRNAs (miR-139-5p and miR-155-5p) were curated for SMARCA4 (Figure 4c). We used GEPIA2 to determine expression profiles of CDK1 in human tumors. The results showed that CDK1 was

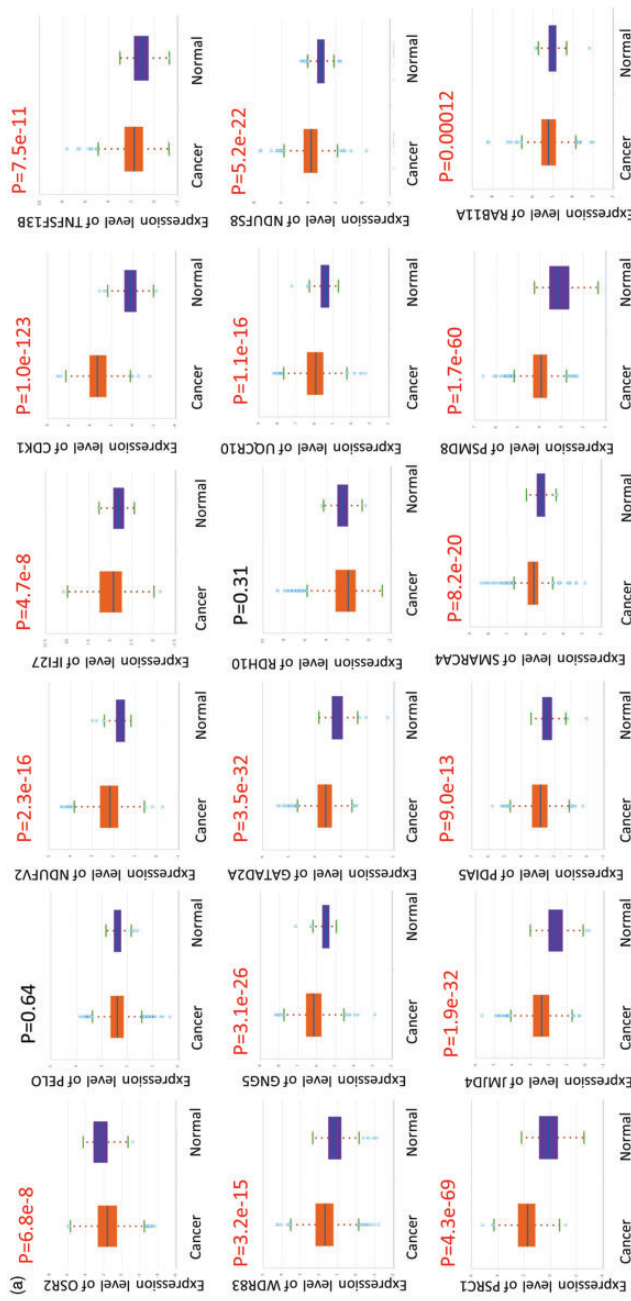


Figure 3. Differential gene expression (a) and survival analyses (b) were performed using the starBase online platform.

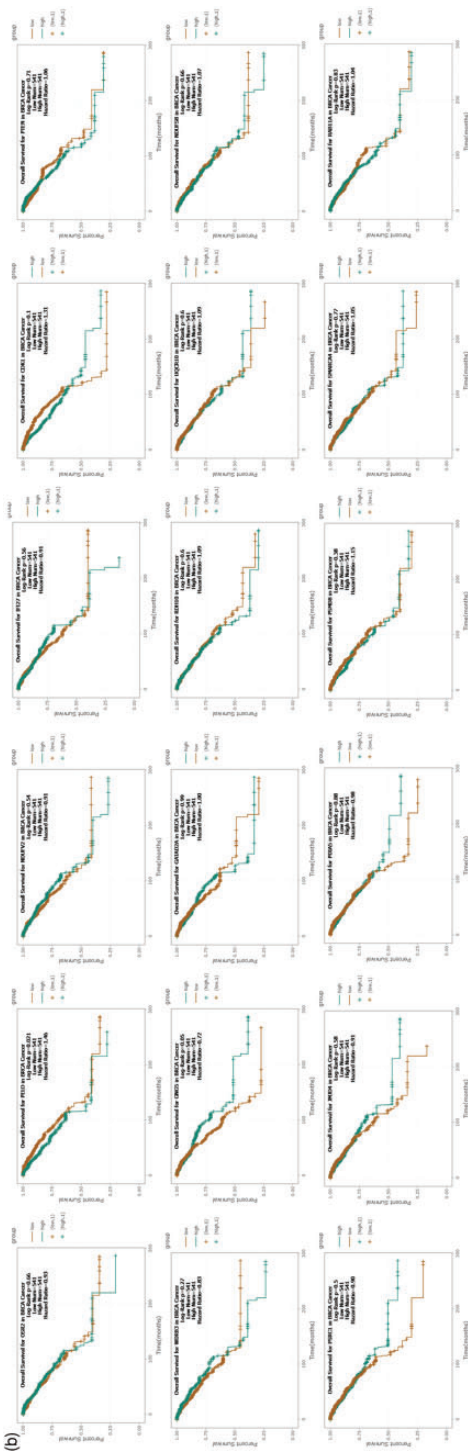


Figure 3. Continued

highly expressed in 21 malignant tumor types relative to matched normal tissues (Figure 5a and b). In contrast, miR-143-3p was markedly downregulated in BC samples relative to normal samples according to starBase data (Figure 6a). Moreover, miR-143-3p expression was negatively correlated with CDK1 levels (Figure 6b). The predicted targets are illustrated in Figure 6c.

MiR-143-3p binds to the 3'UTR of CDK1

A dual-luciferase reporter system was used to determine the relationship between miR-143-3p and CDK1. The results showed that co-transfecting HEK293T cells with a miR-143-3p mimic and the CDK1 3'UTR vector resulted in significantly lower luciferase activity compared with that of cells transfected with the miR negative control and/or CDK1 3'UTR vector alone ($P < 0.01$). Next, we found that luciferase activity was recovered in cells transfected with the CDK1-mut vector ($P < 0.01$) (Figure 7a and b), indicating that miR-143-3p directly targets CDK1 by binding to its 3'UTR.

Validation of CDK1 and miR-143-3p expression in TNBC

Our qPCR results showed that CDK1 was significantly upregulated in 30 TNBC patient samples relative to surrounding tissues ($P < 0.05$) (Figure 8a). Clinicopathological associations between CDK1 and miR-143-3p expression in TNBC are presented in Table 4. In summary, miR-143-3p showed reduced expression in samples from 40 TNBC patient samples relative to surrounding tissues ($P < 0.05$) (Figure 8b). A negative correlation ($p < 0.05$) was observed between miR-143-3p and Ki67 expression (Figure 8c).

Discussion

Recent statistics have revealed that BC is the most prevalent malignant tumor in

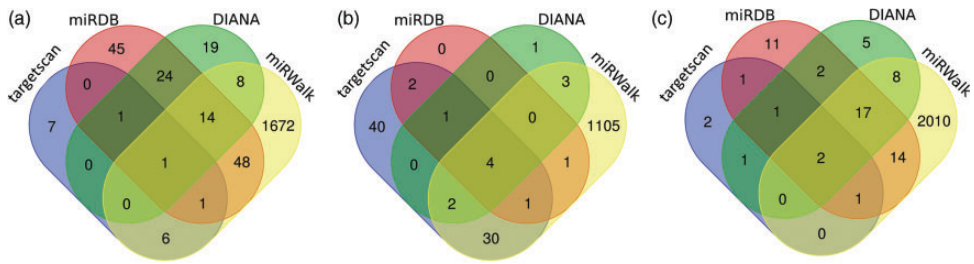


Figure 4. Venn diagram showing the intersection of gene targets for CDK1 (a), IFI27 (b), and SMARCA4 (c). CDK1, cyclin dependent kinase I; IFI27, interferon alpha inducible protein 27; SMARCA4, SWI/SNF related, matrix associated, actin dependent regulator of chromatin, subfamily a, member 4.

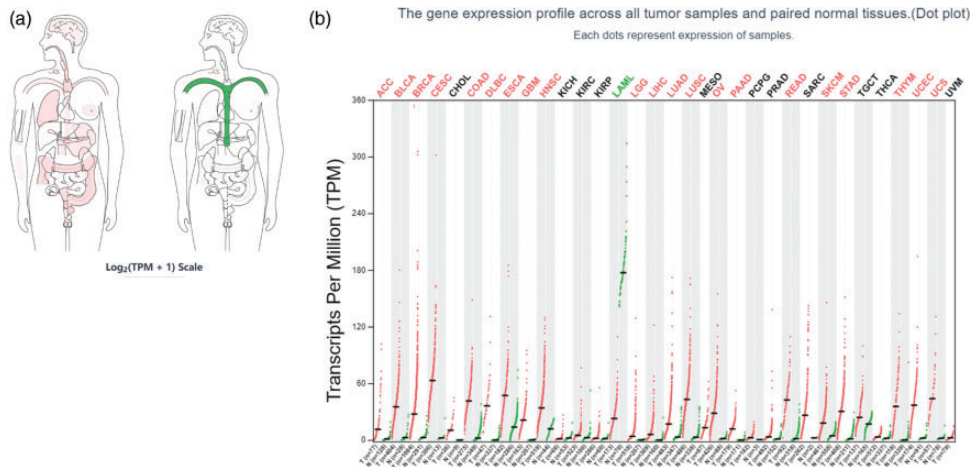


Figure 5. (a) Interactive Body Map. Median expression of tumor and normal samples in Body Map and (b) Gene expression profiles across all tumors relative to paired normal tissues (Bar plot). The height of each bar represents median expression in a particular tumor type or normal tissue.

women, accounting for 30% of all female cancers.¹ The incidence of BC in China has been increasing over recent years,⁷ a complex phenomenon that has been attributed to numerous factors. The familial clusters and ethnic disparities suggest that genetic mutations play a central role in BC-related carcinogenesis.⁸ Therefore, targeted therapy may have great implications for the treatment of BC. The development of targeted therapies for TNBC is challenging due to the lack of expressed targetable receptors, a situation that has made the disease become the most aggressive BC subtype. Moreover, discovering potential

genetic mutations remains a huge challenge for targeted therapy.⁹ Microarray technology has rapidly evolved over the past decade, a phenomenon that has markedly improved explorations of genetic alterations in TNBC.

In this study, we identified 28 DEGs between TNBC and healthy samples across three microarray datasets in the GEO database, of which 10 and 18 were down- and up-regulated, respectively. We performed GO analysis to explore interactions among the upregulated DEGs and found that all 18 were enriched in cell metabolic process and gene expression.

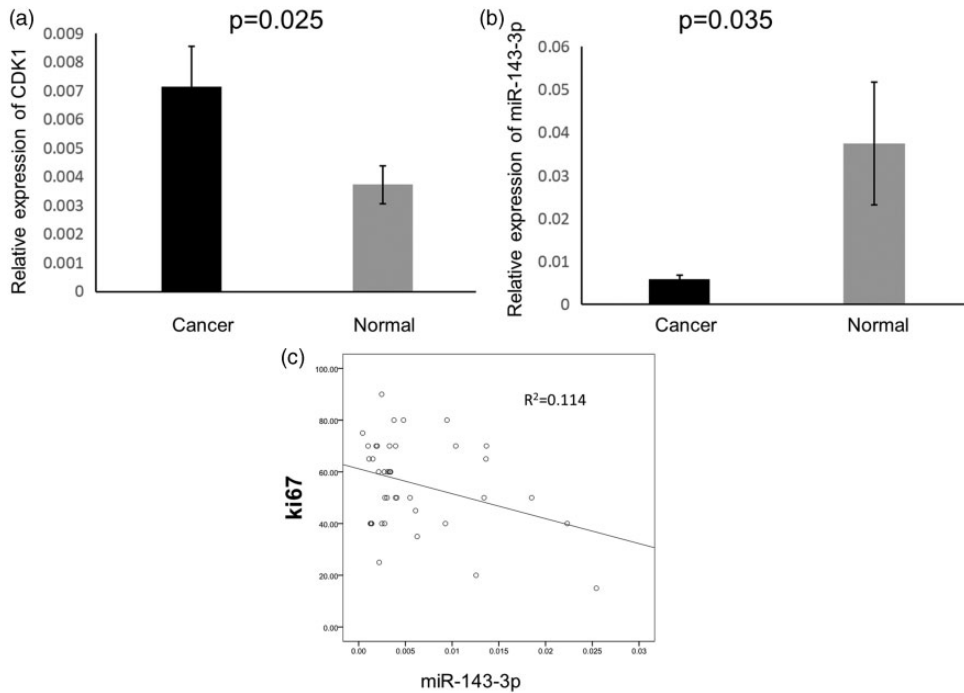


Figure 8. (a) Profile of CDK1 expression in TNBC relative to adjacent normal tissue samples from 30 patients. (b) MiR-143-3p expression in TNBC tissues alongside their adjacent normal tissues across 40 patients and (c) MiR-143-3p expression was correlated with Ki67 (Pearson correlation, $r = 0.114$, $P < 0.05$). CDK1, cyclin dependent kinase I; TNBC, triple-negative breast cancer.

Table 4. Clinicopathologic associations with CDK1 and miR-143-3p in TNBC (n = 45).

Clinical information		Total no.	miR-143	CDK1
Age (years)	≤50	18	15	12
	>50	27	25	18
P-value			0.438	0.492
Tumor size	≤2 cm (T1)	17	16	13
	>2 cm (T2-T3)	28	24	17
P-value			0.092	0.715
Lymph node metastasis	0 (N0)	30	28	21
	≥1 (N1-N3)	15	12	9
P-value			0.35	0.052
Stage	I	15	14	12
	II-III	30	26	18
P-value			0.095	0.86
Ki67	<50%	11	11	7
	≥50%	34	29	23
P-value			0.33	0.771

Functional analysis indicated that the up-regulated DEGs were involved in cell division, mitochondrion, and respiratory chain. Metabolic reprogramming of cancer plays an important role in tumor development.¹⁰ Previous studies have also shown that increased levels of cell cycle-related proteins are correlated with worse survival in BC patients.¹¹ A recent study demonstrated that mitochondria are a potential target for drug resistance in TNBC,¹² while another revealed that inhibiting mitochondrial oxidative phosphorylation prevented tumorigenesis of BC cells without interfering with the metabolism of non-cancerous cells.¹³ Taken together, these observations are consistent with our results. Recently, a new drug that targets TROP-2 named sacituzumab govitecan (SG) was approved for TNBC.¹⁴ Further studies showed that the median overall survival was 12.1 months with SG compared with only 6.7 months with chemotherapy in patients with relapsed or refractory TNBC.¹⁵ Thus, survival was significantly increased with SG compared with chemotherapy among patients with relapsed or refractory TNBC. Therefore, searching for new potential therapeutic targets, biomarkers, and related pathways in TNBC is imperative to improving the management of this disease.

We used miRDB, TargetScan, miRWalk, and DIANA to screen for relevant miRNA–gene interactions and found that only miR-143-3p was associated with CDK1 expression. Members of the CDK family play a key role in cell cycle progression, and CDK1 is considered the best CDK target for BC therapy.^{16,17} Previous studies have shown that CDK1 is regulated by multiple factors, key among them being KIAA1429, which promotes tumor progression.¹⁸ Another study demonstrated that downregulation of NUSAP1 inhibited the tumorigenicity of BC cells by regulating CDK1 expression,¹⁹ while the

miR-143-3p/CDK1 axis has also been found to regulate apoptosis in lung cancer cells.²⁰ Moreover, overexpressing miR-143-3p inhibited the progression of cervical cancer, while CDK1 offset this effect.²¹ However, until now, the relationship between miR-143-3p and CDK1 had not been reported in TNBC. Our results also revealed that miR-139-5p and miR-155-5p were associated with SMARCA4 across all four databases. Studies have not only found that SMARCA4 (also called BRG1) is associated with tumor immunity,²² but is also a key factor for tumor cell proliferation.²³ Notably, the IFI27 gene was associated with miR-5002-5p, miR-6513-5p, miR-942-5p, and miR-6780a-3p. A previous study found that IFI27 overexpression was associated with overall survival in estrogen receptor-positive BC patients.²⁴

Next, we validated CDK1 and miR-143-3p expression using qPCR and found that CDK1 was upregulated, while miR-143-3p was downregulated in TNBC relative to adjacent normal tissues. These results were consistent with previous studies, which have also reported a downregulation of miR-143-3p in clinical BC samples and BC cells.^{25,26} Results from cellular experiments have also demonstrated that increased miR-143-3p expression has antitumor effects in BC cells.²⁷ Functionally, miR-143-3p regulates BC cell proliferation and apoptosis by targeting MYB proto-oncogene like 2.²⁸ Li et al.²⁹ found that miR-143-3p expression improved the sensitivity of BC cells to radiation through fibroblast growth factor-1. Collectively, we hypothesize that miR-143-3p could be involved in multiple signaling pathways by targeting different genes in BC. Moreover, CDK1 participates in the tumorigenesis of TNBC *via* miR-143-3p.

Our results further indicated that miR-143-3p was negatively correlated with Ki67 expression. Generally, higher Ki67 expression is associated with shorter median survival times in BC patients.³⁰

Therefore, these results further affirmed that miR-143-3p is involved in TNBC development. It is possible that lower miR-143-3p expression may be strongly correlated with TNBC malignancy, whereas CDK1 upregulation plays a role in TNBC development. These findings present crucial targets for BC therapy and have significant implications. However, further studies are needed to elucidate the biological functions and pathways regulated by these genes in BC. Our findings further demonstrated that miR-143-3p targets CDK1. This pathway is involved in tumorigenesis in TNBC. However, further validation using *in vitro* and *in vivo* experiments is required before application in clinical practice. Overall, the findings of this study will set a platform for future research that aims to develop therapeutic and diagnostic strategies for TNBC.

Conclusions

This study revealed key genes involved in TNBC development, of which 18 were significantly upregulated in disease samples. CDK1 was found to be associated with miRNAs, suggesting that these could be therapeutic targets for TNBC. Future studies are expected to elucidate the mechanisms underlying the expression changes and biological functions of CDK1 and miR-143-3p in TNBC.

Authors' contributions

Q.N. and C.P. conceptualized and designed the study; Q.N. and A.H. performed experiments; C. P. analyzed data and interpreted experimental results; Q.N. prepared figures and drafted the manuscript; C.P. and A.H. edited and revised the manuscript. All authors approved the final version of the manuscript.

Data availability statement

Data that support the findings of this study are available from the corresponding author upon reasonable request.

Declaration of conflicting interests

The authors declare that the research was conducted in the absence of any commercial or financial relationships.

Funding

The authors disclosed receipt of the following financial support for the research, authorship, and/or publication of this article: This work was supported by funds from the Jiangsu Provincial Double-Innovation Doctor Program (Grant Nos. 202030205 and 202030206).

ORCID iD

Qingtao Ni  <https://orcid.org/0000-0003-0263-5993>

References

1. Siegel RL, Miller KD, Fuchs HE, et al. Cancer Statistics, 2021[J]. *CA Cancer J Clin* 2021; 71: 7–33. DOI:10.3322/caac.21654.
2. Childers CP, Childers KK, Maggard-Gibbons M, et al. National Estimates of Genetic Testing in Women With a History of Breast or Ovarian Cancer[J]. *J Clin Oncol* 2017; 35: 3800–3806. DOI:10.1200/JCO.2017.73.6314.
3. Pataer A, Ozpolat B, Shao R, et al. Therapeutic targeting of the PI4K2A/PKR lysosome network is critical for misfolded protein clearance and survival in cancer cells[J]. *Oncogene* 2020; 39: 801–813. DOI:10.1038/s41388-019-1010-4.
4. Mendes C, Lopes-Coelho F, Ramos C, et al. Unraveling FATP1, regulated by ER-beta, as a targeted breast cancer innovative therapy[J]. *Sci Rep* 2019; 9: 14107. DOI:10.1038/s41598-019-50531-3.
5. Nachreiner I, Hussain AF, Wullner U, et al. Elimination of HER3-expressing breast cancer cells using aptamer-siRNA chimeras [J]. *Exp Ther Med* 2019; 18: 2401–2412. DOI:10.3892/etm.2019.7753.
6. Kalscheuer S, Khanna V, Kim H, et al. Discovery of HSPG2 (Perlecan) as a Therapeutic Target in Triple Negative Breast Cancer[J]. *Sci Rep* 2019; 9: 12492. DOI:10.1038/s41598-019-48993-6.
7. Hao S, Zhao YY, Peng JJ, et al. Invasive micropapillary carcinoma of the breast had

- no difference in prognosis compared with invasive ductal carcinoma: a propensity-matched analysis[J]. *Sci Rep* 2019; 9: 286. DOI:10.1038/s41598-018-36362-8.
8. Wang L, Zhou S, Xie J, et al. BRCA1 germline mutations dominate familial breast cancer patients in Henan China[J]. *J Thorac Dis* 2017; 9: 5295–5299. DOI:10.21037/jtd.2017.11.71.
 9. Gu G, Dustin D and Fuqua SA. Targeted therapy for breast cancer and molecular mechanisms of resistance to treatment[J]. *Curr Opin Pharmacol* 2016; 31: 97–103. DOI:10.1016/j.coph.2016.11.005.
 10. El-Sahli S and Wang L. Cancer Stem Cell-Associated Pathways in the Metabolic Reprogramming of Breast Cancer[J]. *Int J Mol Sci* 2020; 21: 9125. DOI:10.3390/ijms21239125.
 11. Cheng L, Huang YZ, Chen WX, et al. Cell division cycle proteininising prognostic biomarker of breast cancer[J]. *Biosci Rep* 2020; 40: BSR20191227. DOI:10.1042/BSR20191227.
 12. Andreidesz K, Szabo A, Kovacs D, et al. Cytostatic Effect of a Novel Mitochondria-Targeted Pyrroline Nitroxide in Human Breast Cancer Lines[J]. *Int J Mol Sci* 2021; 22: 9016. DOI:10.3390/ijms22169016.
 13. Zhang J, Yan L, Wei P, et al. PEG-GO@XN nanocomposite suppresses breast cancer metastasis via inhibition of mitochondrial oxidative phosphorylation and blockade of epithelial-to-mesenchymal transition[J]. *Eur J Pharmacol* 2021; 895: 173866. DOI:10.1016/j.ejphar.2021.173866.
 14. Coates JT, Sun S, Leshchiner I, et al. Parallel Genomic Alterations of Antigen and Payload Targets Mediate Polyclonal Acquired Clinical Resistance to Sacituzumab Govitecan in Triple-Negative Breast Cancer[J]. *Cancer Discov* 2021; 11: 2436–2445. DOI:10.1158/2159-8290.CD-21-0702.
 15. Bardia A, Hurvitz SA, Tolaney SM, et al. Sacituzumab Govitecan in Metastatic Triple-Negative Breast Cancer[J]. *N Engl J Med* 2021; 384: 1529–1541. DOI:10.1056/NEJMoa2028485.
 16. Izadi S, Nikkhoo A, Hojjat-Farsangi M, et al. CDK1 in Breast Cancer: Implications for Theranostic Potential[J]. *Anticancer Agents Med Chem* 2020; 20: 758–767. DOI:10.2174/1871520620666200203125712.
 17. Lu Y, Yang G, Xiao Y, et al. Upregulated cyclins may be novel genes for triple-negative breast cancer based on bioinformatic analysis[J]. *Breast Cancer* 2020; 27: 903–911. DOI:10.1007/s12282-020-01086-z.
 18. Qian JY, Gao J, Sun X, et al. KIAA1429 acts as an oncogenic factor in breast cancer by regulating CDK1 in an N6-methyladenosine-independent manner[J]. *Oncogene* 2019; 38: 6123–6141. DOI:10.1038/s41388-019-0861-z.
 19. Zhang X, Pan Y, Fu H, et al. Nucleolar and Spindle Associated Protein 1 (NUSAP1) Inhibits Cell Proliferation and Enhances Susceptibility to Epirubicin In Invasive Breast Cancer Cells by Regulating Cyclin D Kinase (CDK1) and DLGAP5 Expression[J]. *Med Sci Monit* 2018; 24: 8553–8564. DOI:10.12659/MSM.910364.
 20. Li Q, Bian Y and Li Q. Down-Regulation of TMPO-AS1 Induces Apoptosis in Lung Carcinoma Cells by Regulating miR-143-3p/CDK1 Axis[J]. *Technol Cancer Res Treat* 2021; 20. DOI:10.1177/1533033820948880.
 21. Tang J, Pan H, Wang W, et al. MiR-495-3p and miR-143-3p co-target CDK1 to inhibit the development of cervical cancer[J]. *Clin Transl Oncol* 2021; 23: 2323–2334. DOI:10.1007/s12094-021-02687-6.
 22. Peng L, Li J, Wu J, et al. A Pan-Cancer Analysis of SMARCA4 Alterations in Human Cancers[J]. *Front Immunol* 2021; 12: 762598. DOI:10.3389/fimmu.2021.762598.
 23. Wu Q, Madany P, Akech J, et al. The SWI/SNF ATPases Are Required for Triple Negative Breast Cancer Cell Proliferation [J]. *J Cell Physiol* 2015; 230: 2683–2694. DOI:10.1002/jcp.24991.
 24. Cervantes-Badillo MG, Paredes-Villa A, Gomez-Romero V, et al. IFI27/ISG12 Downregulates Estrogen Receptor alpha Transactivation by Facilitating Its Interaction With CRM1/XPO1 in Breast Cancer Cells[J]. *Front Endocrinol (Lausanne)* 2020; 11: 568375. DOI:10.3389/fendo.2020.568375.
 25. Fattahi DN, Dehghani A, Shahand E, et al. The interaction between MALAT1 target, miR-143-3p, and RALGAPA2 is affected by functional SNP rs3827693 in breast

- cancer[J]. *Hum Cell* 2020; 33: 1229–1239. DOI:10.1007/s13577-020-00422-x.
26. Xia C, Yang Y, Kong F, et al. MiR-143-3p inhibits the proliferation, cell migration and invasion of human breast cancer cells by modulating the expression of MAPK7[J]. *Biochimie* 2018; 147: 98–104. DOI:10.1016/j.biochi.2018.01.003.
27. Guo Y, Liang F, Zhao F, et al. Resibufogenin suppresses tumor growth and Warburg effect through regulating miR-143-3p/HK2 axis in breast cancer[J]. *Mol Cell Biochem* 2020; 466: 103–115. DOI:10.1007/s11010-020-03692-z.
28. Chen J and Chen X. MYBL2 Is Targeted by miR-143-3p and Regulates Breast Cancer Cell Proliferation and Apoptosis[J]. *Oncol Res* 2018; 26: 913–922. DOI:10.3727/096504017X15135941182107.
29. Wang D, Wang C, Sun L, et al. MiR-143-3p Increases the Radiosensitivity of Breast Cancer Cells Through FGF1[J]. *Cell Mol Biol (Noisy-le-grand)* 2022; 67: 256–262. DOI:10.14715/cmb/2021.67.5.35.
30. Li Y, Zhang X, Qiu J, et al. Comparisons of p53, KI67 and BRCA1 expressions in patients with different molecular subtypes of breast cancer and their relationships with pathology and prognosis[J]. *J BUON* 2019; 24: 2361–2368.